

Polymer microcantilevers fabricated via multiphoton absorption polymerization

Z. Bayindir, Y. Sun, and M. J. Naughton^{a)}

Department of Physics, Boston College, Chestnut Hill, Massachusetts 02467

C. N. LaFratta, T. Baldacchini, and J. T. Fourkas

Department of Chemistry, Boston College, Chestnut Hill, Massachusetts 02467

J. Stewart, B. E. A. Saleh, and M. C. Teich

Department of Electrical Engineering, Boston University, Boston, Massachusetts 02215

(Received 28 June 2004; accepted 14 December 2004; published online 3 February 2005)

We have used multiphoton absorption polymerization to fabricate a series of microscale polymer cantilevers. Atomic force microscopy has been used to characterize the mechanical properties of microcantilevers with spring constants that were found to span more than four decades. From these data, we extracted a Young's modulus of $E=0.44$ GPa for these microscale cantilevers. The wide stiffness range and relatively low elastic modulus of the microstructures make them attractive candidates for a range of microcantilever applications, including measurements on soft matter.

© 2005 American Institute of Physics. [DOI: 10.1063/1.1863414]

Multiphoton absorption polymerization (MAP)^{1–4} offers the unparalleled ability to create arbitrarily complex 3D polymeric structures with a resolution that can be in the range of 100 nm.⁵ Structures created using MAP may find use in a broad range of micromechanical and microfluidic applications spanning the physical and biological sciences. As such, there is great interest in understanding how the mechanical properties of structures created with MAP compared to those of structures created from the same materials via conventional photopolymerization. In the one reported study on this topic to date, the force constant of a polymeric spring fabricated via MAP was estimated by two different methods to be between *three and five orders of magnitude smaller* than would be predicted from the properties of the bulk polymer.⁶ If correct, this surprising result has significant implications for the creation of functional microstructures with MAP. In this letter, we examine this issue by making force measurements on microscopic cantilevers fabricated from a similar polymer using MAP. We find that the Young's modulus of the cantilevers is of the same order of magnitude as that of the bulk polymer and demonstrate that transparent microcantilevers with spring constants spanning a broad stiffness range ($<10^{-2}$ – 10^2 N/m) can be fabricated readily with MAP.

MAP fabrication^{7,8} is achieved in our case with a focused ultrafast laser beam centered at 800 nm, a wavelength to which liquid acrylic prepolymer resins are transparent. Pairs of photons cause local polymerization within the tight focal volume of the beam. The center point of this voxel is translated in the x , y , and z directions using a motorized microscope stage, creating positive solid 3D structures of preprogrammed shape in the resin. Unpolymerized material is washed away when the fabrication is complete, leaving behind the desired structures (cantilevers, in this instance). Our prepolymer resin is composed of equal parts SR-499, ethoxylated trimethylolpropanetriacrylate (Sartomer), and SR-368, tris(2-hydroxyethyl)isocyanurate triacrylate (Sar-

tomer), with 3% wt. Lucirin-TPOL, 2,4,6-trimethylbenzoylthoxyphenylphosphine oxide (BASF) employed as a photoinitiator. The preparation of the samples for photopolymerization and the experimental setup used are explained in detail elsewhere.⁹ At present, our system can create structures with features sizes under 200 nm. Examples of complex microstructures made by this method can be found in Refs. 10 and 11.

To fabricate MAP microcantilevers, we begin by preparing a rectangular base structure from the same polymer, either in bulk form via conventional photopolymerization or by the MAP process. Using MAP, the microcantilever is then fabricated such that it extends from this base. A SEM image of a polymer cantilever, along with a closeup of its surface, is shown in Fig. 1. The surface roughness is on the submicron scale, although ridges due to a longer dwell time at turning points of the stage are visible at the edges of the cantilever.

We have fabricated a number of such cantilevers with a different physical dimensions, and thus with different me-

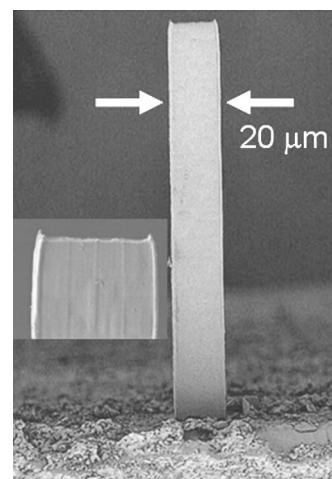


FIG. 1. SEM image of a $4\ \mu\text{m}$ thick $\times 20\ \mu\text{m}$ wide $\times 155\ \mu\text{m}$ tall polymer cantilever fabricated by MAP. The inset is a closer view of the surface of the cantilever. A film of gold was evaporated to facilitate SEM imaging. As prepared, these devices are transparent to visible light.

^{a)}Electronic mail: naughton@bc.edu

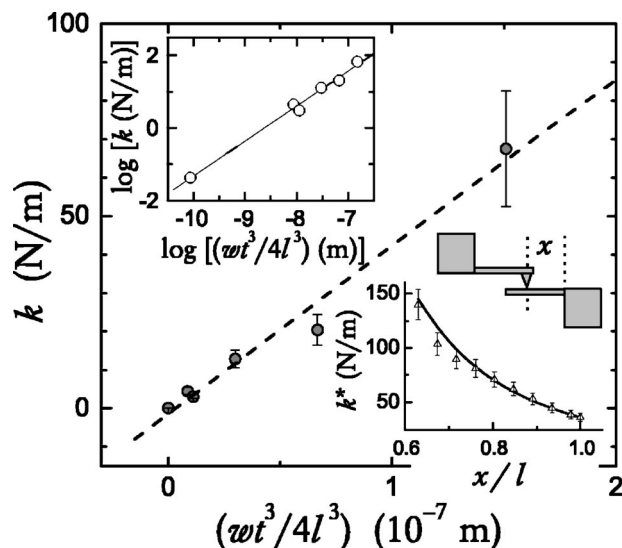


FIG. 2. Spring constants k of MAP-fabricated polymer cantilevers vs size parameter $(w/4)(t/l)^3$, showing correspondence across several decades. The slope is the Young's modulus of the polymer. Left inset: same data on log scales. Right inset: Effective spring constant k^* of a Si AFM cantilever vs point of contact x along the cantilever length (total length ℓ), used to verify the AFM method employed, and sketched at right.

chanical properties. Typical dimensions are $100 \mu\text{m}$ long $\times 20 \mu\text{m}$ wide $\times 10 \mu\text{m}$ thick. The stiffness of a cantilever with a uniform rectangular cross section can be expressed by its spring constant, k , which is given by $k = Ewt^3/4\ell^3$, where E is the Young's elastic modulus of the material, and w , t , and ℓ are the width, thickness, and length of the cantilever, respectively. In order to characterize the mechanical properties of microstructures prepared by this multiphoton process, we measured the spring constants of a number of cantilevers, and extracted E from these measurements.

We used the force-distance feature of a commercial AFM¹² (Veeco / DI Dimension 3100) to measure the cantilever spring constants. In this technique, a "sample" cantilever fabricated by MAP is deflected with a calibrated AFM cantilever, as shown in the schematic inset to Fig. 2. We first measured the effective spring constant of a polymeric cantilever as a function of the point of contact x along its length. We employed two different calibrated cantilevers (Mikromash Model NSC16-F) with quoted spring constants of 40.9 and 38.9 N/m ($\pm 10\%$). The force-displacement feature of the AFM itself was calibrated by pressing on a noncompliant surface (e.g., a silicon substrate) with a cantilever of known spring constant.

Upon mutual deflection, the forces acting on the two cantilevers arranged as in Fig. 2 are equal, $k_1d_1 = k_2d_2$, where 1 and 2 refer to the known and unknown cantilevers, and the d 's are the corresponding vertical deflections of these cantilevers. The AFM used for our experiment measures the deflection of the known cantilever as a function of the change in the z -axis piezoelectric crystal, d_p , and the sum of the sample cantilever deflection and AFM cantilever deflection gives the change in this piezo, $d_p = d_1 + d_2$. Using the slope m of a d_1 vs d_p plot, we can write $k_2 = k_1m/(1-m)$, giving the quantity we desire (k_2) in terms of known (k_1) or measured (m) quantities. By this method, we measured a spring constant of 36.2 ± 0.4 N/m for the above "38.9 N/m" cantilever, clearly within the manufacturer's 10% uncertainty. As can be seen from the lower right inset in Fig. 2, the measured spring

TABLE I. Dimensions (thickness t , width w , and length ℓ) and measured spring constants k with their uncertainties for six cantilevers fabricated by MAP and characterized via AFM. Also shown are calculated spring constants using the Young's modulus derived from the data. Only the calculated spring constant is given for the device on the top line.

t (μm)	w (μm)	ℓ (μm)	k_{calc} (N/m)	k_{meas} (N/m)	$\delta k/k$ (%)
5.0	8.3	260.3	0.0065	-	-
4.0	20.0	155.0	0.04	0.04	25
15.0	19.5	113.7	3.9	3.0	16
10.6	19.8	87.4	4.9	4.5	20
17.1	29.8	107.3	13.3	12.9	18
20.1	29.5	96.4	29.4	20.4	20
14.3	29.1	51.9	67.0	67.5	32

constant follows the theoretical $k \sim x^{-3}$ curve, especially as the contact point is moved closer to the end of the tested cantilever ($x = \ell$). Deviations arise for smaller values of x , possibly because of an anharmonic response.

These results showed that the force-distance feature of the AFM can be utilized for spring constant measurements, allowing us to then measure the spring constants of our polymer cantilevers. Using this technique, we measured the spring constants of several polymer cantilevers having different dimensions. Table I shows a list of cantilevers with their dimensions and measured spring constants. About half of the uncertainty in this latter quantity stems from the 10% uncertainty in the spring constants of the commercially calibrated cantilevers used in the measurements.

In Fig. 2, we plot on linear (main plot) and log-log (upper inset) scales the six measured spring constants in Table I versus $(w/4)(t/\ell)^3$, as calculated from the table. It is important to note that the force constant is observed to vary linearly with $(w/4)(t/\ell)^3$ over the rather broad range of cantilever dimensions that were investigated, suggesting that finite-size effects do not play a role in determining the elastic properties of the cantilevers on these size scales. The slope of the linear plot implies a Young's modulus of $E = 0.44 \pm 0.03$ GPa. Using this value, in Table I we also show the calculated spring constants for the tested cantilevers. A seventh device's dimensions were recorded by SEM, but this one proved too soft for its spring constant to be measured reliably via the AFM method above. Thus, the only k given in the table is that calculated with the use of the derived Young's modulus.

The measured Young's modulus is nearly an order of magnitude smaller than that of SU-8 (Ref. 13) and other such hard polymer materials. In order to investigate this further, we measured the elastic properties of *macroscale* objects made from our acrylic polymer in a single-photon process. Cylinders of 3 mm diameter and 20 mm length, polymerized by white light and tested by an Instron Model 4202 mechanical testing system, yielded a Young's modulus of 2 GPa. Other simple macrostructures tested by nanoindentation gave similar values. These values are about 4 times larger than those of MAP-fabricated cantilevers. As a double check, to ensure that our AFM-derived results were not skewed by the sharp AFM tip indenting the compliant polymer surface while bending the cantilever, a nanoindentation experiment performed directly on a two-photon-fabricated microstructure (noncantilever) using the AFM gave a modulus of 0.52 ± 0.11 GPa, confirming our main result.

While the Young's modulus that we measure for MAP cantilevers differs significantly from that of the bulk polymer, the magnitude of this discrepancy is plausible and is far smaller than that found previously.⁶ Since the previous experiments⁶ were conducted in a liquid, it is possible that Reynold's number considerations were not taken into account properly. We are continuing to investigate the difference in Young's modulus between polymers created conventionally and with MAP, and we suspect that this effect is due at least in part to the fact that MAP hardens the resin on a voxel-by-voxel basis. Not only does each voxel have a high surface-to-volume ratio, but it is also possible for the two components of the resin to disproportionate over the course of polymerization in the small volume of a voxel.

Our studies also underscore the fact that MAP cantilevers may have significant advantages over conventional cantilevers in particular applications. The range of spring constants of our MAP cantilevers covers most of that used in the commercial AFM market. Our polymer is more than 400 times softer than Si and close to 1000 times softer than Si₃N₄, based on Young's moduli¹⁴ ($E_{\text{Si}}=190$ GPa and $E_{\text{Si}_3\text{N}_4}\sim 400$ GPa), which allows us to fabricate much softer cantilevers that may be of use in studies of soft condensed matter.

MAP cantilevers offer considerably more freedom in design than do Si-based cantilevers; for instance, cantilevers with nonuniform thickness, which can have favorable thermal noise characteristics,¹⁵ are no more difficult to create with MAP than are ones with uniform thickness. In addition, MAP polymer cantilevers are optically transparent (unlike Si) and are easily functionalized, features that can be exploited to investigate biosensing or optical functionalities.

In summary, we have used a series of microcantilevers created via multiphoton absorption polymerization to measure the Young's modulus of an acrylic polymer. While the elastic modulus of the MAP material is smaller than that of the bulk polymer, the difference is only about a factor of

four. A broad range of force constants is accessible with MAP cantilevers of reasonable dimensions, and the MAP technique offers complete flexibility in the design of microcantilevers.

The authors acknowledge financial support from NSF "XYZ-on-a-Chip" and NIRT Programs, Grant Nos. ECS-0088438 and NIRT-0210533. We also thank Professor C. Klapperich for assistance with the nanoindentation experiments. J.T.F. is a Research Corporation Cottrell Scholar and a Camille Dreyfus Teacher-Scholar.

¹S. Maruo, O. Nakamura, and S. Kawata, *Opt. Lett.* **22**, 132 (1997).

²P. J. Campagnola, A. R. Howell, D. Delgudas, J. D. Pitts, and S. L. Goodman, *Macromolecules* **33**, 1511 (2000).

³B. H. Cumpston, S. P. Ananthavel, S. Barlow, D. L. Dyer, J. E. Ehrlich, L. L. Erskine, A. A. Heikal, S. M. Kuebler, I.-Y. Lee, D. McCord-Maughon, J. Qin, H. Rockel, M. Rumi, X.-L. Wu, S. R. Marder, and J. W. Perry, *Nature (London)* **398**, 51 (1999).

⁴G. Witzgall, R. Vrijen, E. Yablonovitch, V. Doan, and B. J. Schwartz, *Opt. Lett.* **23**, 1745 (1998).

⁵S. Kawata, H.-B. Sun, T. Tanaka, and K. Takada, *Nature (London)* **412**, 697 (2001).

⁶H.-B. Sun, K. Takada, and S. Kawata, *Appl. Phys. Lett.* **79**, 3173 (2001).

⁷T. Baldacchini and J. T. Fourkas, in *Encyclopedia of Nano-Science and Nanotechnology*, edited by J. A. Schwarz, C. I. Contescu, and K. Putyera (Marcel Dekker, New York, 2004), p. 3905.

⁸H.-B. Sun and S. Kawata, *J. Lightwave Technol.* **21**, 624 (2003).

⁹T. Baldacchini, H. Chen, R. A. Farrer, M. J. R. Previte, J. Moser, M. J. Naughton, and J. T. Fourkas, *Proc. SPIE* **4633**, 136 (2002).

¹⁰T. Baldacchini, C. LaFratta, R. A. Farrer, M. C. Teich, B. E. A. Saleh, M. J. Naughton, and J. T. Fourkas, *J. Appl. Phys.* **95**, 6072 (2004).

¹¹C. LaFratta, T. Baldacchini, R. A. Farrer, M. C. Teich, B. E. A. Saleh, M. J. Naughton, and J. T. Fourkas, *J. Phys. Chem. B* **108**, 11256 (2004).

¹²A. Torii, M. Sasaki, K. Hane, and S. Okuma, *Meas. Sci. Technol.* **7**, 179 (1996).

¹³MicroChem Corp., 1254 Chestnut St., Newton, MA 02464, www.microchem.com

¹⁴K. Peterson, *Proc. IEEE* **70**, 420 (1982).

¹⁵H. J. Mamin, R. Budakian, B. W. Chui, and D. Rugar, *Phys. Rev. Lett.* **91**, 207604 (2003).